

# Iterative bandgap engineering at selected areas of quantum semiconductor wafers

Radoslaw Stanowski<sup>1</sup>, Matthieu Martin<sup>1</sup>, Richard Ares<sup>2</sup>, and Jan J. Dubowski<sup>1\*</sup>

<sup>1</sup>Department of Electrical and Computer Engineering, Center of Excellence for Information Engineering, Université de Sherbrooke, Sherbrooke, Québec J1K 2R1, Canada

<sup>2</sup>Department of Mechanical Engineering, Center of Excellence for Information Engineering, Université de Sherbrooke, Sherbrooke, Québec J1K 2R1, Canada

\*jan.j.dubowski@usherbrooke.ca

**Abstract:** We report on the application of a laser rapid thermal annealing technique for iterative bandgap engineering at selected areas of quantum semiconductor wafers. The approach takes advantage of the quantum well intermixing (QWI) effect for achieving targeted values of the bandgap in a series of small annealing steps. Each QWI step is monitored by collecting a photoluminescence map and, consequently, choosing the annealing strategy of the next step. An array of eight sites, 280  $\mu\text{m}$  in diameter, each emitting at 1480 nm, has been fabricated with a spectral accuracy of better than 2 nm in a standard InGaAs/InGaAsP QW heterostructure that originally emitted at 1550 nm.

©2009 Optical Society of America

**OCIS codes:** (120.6810) Thermal effects; (140.3390) Laser materials processing; (160.3130) Integrated optics material; (130.3120) Integrated optics devices; (230.5590) Quantum well, - wire and -dot devices.

---

## References and links

1. H. Heidrich, "Monolithically integrated photonic and optoelectronic circuits based on InP - System applications, technology, perspectives," *Microsystem Technol.-Micro-and Nanosystems-Inform, Storage and Proc. Systems* **9**, 295–298 (2003).
2. P. Legay, F. Alexandre, J. L. Benchimol, M. Allovon, F. Laune, and S. Fouchet, "Selective area chemical beam epitaxy for butt-coupling integration," *J. Cryst. Growth* **164**(1-4), 314–320 (1996).
3. K. Kamon, S. Takagishi, and H. Mori, "Selective Embedded Growth of  $\text{Al}_x\text{Ga}_{1-x}\text{As}$  by Low-Pressure Organometallic Vapor-Phase Epitaxy," *Japan. J. Appl. Phys. Letters* **25**(Part 2, No. 1), L10–12 (1986).
4. J. A. Lebens, C. S. Tsai, K. J. Vahala, and T. F. Kuech, "Application of Selective Epitaxy to Fabrication of Nanometer Scale Wire and Dot Structures," *Appl. Phys. Lett.* **56**(26), 2642–2644 (1990).
5. Y. T. Sun, E. R. Messmer, S. Lourduoss, J. Ahopelto, S. Rennon, J. P. Reithmaier, and A. Forchel, "Selective growth of InP on focused-ion-beam-modified GaAs surface by hydride vapor phase epitaxy," *Appl. Phys. Lett.* **79**, 1885–1887 (2001).
6. N. Tamura, and Y. Shimamune, "45 nm CMOS technology with low temperature selective epitaxy of SiGe," *Appl. Surf. Sci.* **254**(19), 6067–6071 (2008).
7. N. Otsuka, M. Kito, Y. Mori, M. Ishino, and Y. Matsui, "New Structure by Selective Regrowth in Multiquantum-Well Laser-Diodes Performed by Low-Pressure Metalorganic Vapor-Phase Epitaxy," *J. Cryst. Growth* **145**(1-4), 866–874 (1994).
8. C. A. Verschuren, P. J. Harmsma, Y. S. Oei, M. R. Leys, H. Vonk, and J. H. Wolter, "Butt-coupling loss of 0.1 dB/interface in InP/InGaAs MQW waveguide-waveguide structures grown by selective area chemical beam epitaxy," *J. Cryst. Growth* **188**(1-4), 288–294 (1998).
9. K. A. Anselm, W. Y. Hwang, H. W. Ren, D. Zhang, and J. Um, "Manufacturing of laser diodes grown by molecular beam epitaxy for coarse wavelength division multiplexing systems," *J. Vac. Sci. Technol. B* **26**(3), 1167–1170 (2008).
10. T. Sasaki, M. Yamaguchi, and M. Kitamura, "Monolithically Integrated Multiwavelength Mqw Dbr Laser-Diodes Fabricated by Selective Metalorganic Vapor-Phase Epitaxy," *J. Cryst. Growth* **145**(1-4), 846–851 (1994).
11. K. Kudo, K. Yashiki, T. Sasaki, Y. Yokoyama, K. Hamamoto, T. Morimoto, and M. Yamaguchi, "1.55- $\mu\text{m}$  wavelength-selectable microarray DFB-LD's with monolithically integrated MMI combiner, SOA, and EA-Modulator," *IEEE Photon. Technol. Lett.* **12**(3), 242–244 (2000).
12. N. Kashio, K. Kurishima, K. Sano, M. Ida, N. Watanabe, and H. Fukuyama, "Monolithic integration of InP HBTs and uni-traveling-carrier photodiodes using nonselective regrowth," *IEEE Trans. Electron. Dev.* **54**(7), 1651–1657 (2007).

13. Y. Suzuki, H. Yasaka, H. Mawatari, K. Yoshino, Y. Kawaguchi, S. Oku, R. Iga, and H. Okamoto, "Monolithically integrated eight-channel WDM modulator with narrow channel spacing and high throughput," *IEEE J. Sel. Top. Quantum Electron.* **11**(1), 43–49 (2005).
14. R. L. Thornton, R. D. Burnham, T. L. Paoli, N. Holonyak, and D. G. Deppe, "Highly Efficient, Long Lived AlGaAs Lasers Fabricated by Silicon Impurity Induced Disorder," *Appl. Phys. Lett.* **49**(3), 133–134 (1986).
15. E. H. Li, *Selected papers on quantum well intermixing for photonics*, Bellingham, Wash.: SPIE Optical Engineering Press, 1998.
16. J. Beauvais, J. H. Marsh, A. H. Kean, A. C. Bryce, and C. Button, "Suppression of Bandgap Shifts in GaAs/AlGaAs Quantum-Wells Using Strontium Fluoride Caps," *Electron. Lett.* **28**(17), 1670–1672 (1992).
17. J. H. Marsh, O. P. Kowalski, S. D. McDougall, B. C. Qiu, A. McKee, C. J. Hamilton, R. M. De la Rue, and A. C. Bryce, "Quantum well intermixing in material systems for 1.5  $\mu\text{m}$  (invited)," *J. Vac. Sci. Technol. A* **16**(2), 810–816 (1998).
18. E. J. Skogen, J. W. Raring, G. B. Morrison, C. S. Wang, V. Lal, M. L. Masanovic, and L. A. Coldren, "Monolithically integrated active components: A quantum-well intermixing approach," *IEEE J. Sel. Top. Quantum Electron.* **11**(2), 343–355 (2005).
19. A. McKee, C. J. McLean, G. Lullo, A. C. Bryce, R. M. DeLaRue, J. H. Marsh, and C. C. Button, "Monolithic integration in InGaAs-InGaAsP multiple-quantum-well structures using laser intermixing," *IEEE J. Quantum Electron.* **33**(1), 45–55 (1997).
20. J. J. Dubowski, C. N. Allen, and S. Fafard, "Laser-induced InAs/GaAs quantum dot intermixing," *Appl. Phys. Lett.* **77**(22), 3583–3585 (2000).
21. J. J. Dubowski, Y. Feng, P. J. Poole, M. Buchanan, S. Poirier, J. Genest, and V. Aimez, "Monolithic multiple wavelength ridge waveguide laser array fabricated by Nd:YAG laser-induced quantum well intermixing," *J. Vac. Sci. Technol. A* **20**(4), 1426–1429 (2002).
22. J. J. Dubowski, C. Y. Song, J. Lefebvre, Z. Wasilewski, G. Aers, and H. C. Liu, "Laser-induced selective area tuning of GaAs/AlGaAs quantum well microstructures for two-color IR detector operation," *J. Vac. Sci. Technol. A* **22**(3), 887–890 (2004).
23. R. Stanowski, O. Voznyy, and J. J. Dubowski, "Finite element model calculations of temperature profiles in Nd:YAG laser annealed GaAs/AlGaAs quantum well microstructures," *J. Laser Micro Nanoengineering* **1**, 17–21 (2006).
24. J. Genest, R. Beal, V. Aimez, and J. J. Dubowski, "ArF laser-based quantum well intermixing in InGaAs/InGaAsP heterostructures," *Appl. Phys. Lett.* **93**(7), 071106 (2008).
25. T. Biondi, A. Scuderi, E. Ragonese, and G. Palmisano, "Characterization and modeling of silicon integrated spiral inductors for high-frequency applications," *Analog Integr. Circ. Sig. Process.* **51**(2), 89–100 (2007).
26. R. Stanowski, and J. J. Dubowski, "Laser rapid thermal annealing of quantum semiconductor wafers: a one step bandgap engineering technique," *Appl. Phys., A Mater. Sci. Process.* **94**(3), 667–674 (2009).
27. R. Stanowski, S. Bouazis, and J. J. Dubowski, "Selective area bandgap engineering of InGaAsP/InP quantum well microstructures with an infrared laser rapid thermal annealing technique," *Proc. SPIE, Vol.*, vol. **6869**, 68790D (2008).
28. L. Lu, A. Mock, M. Bagheri, E. H. Hwang, J. O'Brien, and P. D. Dapkus, "Double-heterostructure photonic crystal lasers with lower thresholds and higher slope efficiencies obtained by quantum well intermixing," *Opt. Express* **16**(22), 17342–17347 (2008).

## 1. Introduction

Bandgap engineering techniques addressing fabrication of the III-V quantum semiconductor (QS) wafers with spatially selected regions of different bandgap energy material have been of great interest for fabrication of monolithically integrated photonic devices (MIPDs) [1-2]. The natural approaches to spatially modify the bandgap of a QS wafer are based on selective area epitaxy [3–6] and selective etch-re-growth [7–9]. Fabrication of numerous MIPDs has been demonstrated with these techniques [10–13]. However, the difficult to control quality of etched surfaces and fabricated interfaces often contributes to low manufacturing yields and, consequently, to the high-cost of devices fabricated with these approaches. The major challenge is to develop a cost-effective process capable of delivering multibandgap QS wafers with both high spectral and spatial accuracy. Since the pioneering works of early 80's that introduced the concept of impurity-enhanced selected area intermixing of the barrier and quantum well materials, known as quantum well intermixing (QWI) [14], this approach has been studied intensively to address fabrication of MIPDs [15–18]. High-temperature annealing is the basis of any QWI technique, thus the choice of a laser as a heating source in this process is attractive due to the ease with which a laser beam can be delivered to a well defined spot [19–24]. Despite these advancements, the spectral accuracy of the QWI process has remained poorly defined, primarily due to the difficult technology of III-V materials that

has prevented the introduction of bandgap engineering processes relying on accurate calibration procedures, analogous to those known in the manufacture of Si-based circuits comprising, e.g., a monolithically integrated inductance [25].

To address this issue, we have developed a highly-reproducible process of iterative bandgap engineering at selected areas (IBESA) that allows fabrication of QS wafers with regions of QWI material emitting at arbitrarily set blue-shifted wavelengths.

## 2. Experimental details

The spatially selective laser annealing of QS wafers was carried out with the laser rapid thermal annealing (Laser-RTA) setup described elsewhere [26]. In short, the procedure is based on using a 150 W 980 nm fiber coupled laser diode (LD) for background heating, and a 30 W TEM00 Nd:YAG laser emitting at a wavelength of 1064 nm for ‘writing’ of regions of the QWI material. The system is equipped with a galvanometric scanner (GS) allowing to raster the Nd:YAG laser beam over the sample with a controlled velocity of 1-4000 mm/s. An F-Theta lens mounted at the output of the GS head assures that a beam with the same profile is delivered to any site of the wafer’s surface. Temperature of the processed spot was monitored with Mikron M680 and a custom designed infrared camera (IR-CAM). Another 640 x 480 pixel visible camera (Vis-CAM) operating at 10 Hz was used to monitor the sample’s positioning. With a 0.5 mm diameter of the Nd:YAG laser spot and depending on the amplitude of the blueshift, the fabrication of QWI material could be carried out with the spatial resolution of 100 to 400  $\mu\text{m}$ . Higher spatial resolution processing is feasible as the Nd:YAG laser beam delivery system allows working with laser spots down to 12  $\mu\text{m}$  in diameter.

The metal-organic vapor phase epitaxial InGaAs/InGaAsP microstructures were grown on a 0.375 mm thick InP substrate covered with a 1.5  $\mu\text{m}$  thick InP buffer layer and a 110 nm thick graded index InGaAsP layer. The microstructure comprised five 6 nm thick InGaAs QWs separated by 10 nm thick InGaAsP barriers. The active region was Si doped at  $8 \times 10^{17} \text{ cm}^{-3}$  and capped with a 20 nm-thick InGaAsP, 40 nm InP, 6 nm InGaAs etch stop layer and topped with a 30 nm thick InP layer. The capping was p-type doped at  $5 \times 10^{17} \text{ cm}^{-3}$ . The room-temperature QW PL emission wavelength from this microstructure was at 1550 nm. The dimensions of a sample used in this study were 10 mm x 12 mm x 0.375 mm. The as-grown wafer was coated with plasma-enhanced-chemical-vapor-deposition 50 and 500 nm thick  $\text{SiO}_2$  layers on the front (polished) and back (unpolished) sides of the wafer, respectively. The  $\text{SiO}_2$  caps prevented the wafers from high-temperature decomposition in the atmospheric environment. Before Laser-RTA processing, the samples were cleaned, sequentially, with OptiClear, Acetone, Isopropyl Alcohol, and finally rinsed with deionized water. The background and intermixing temperatures were set at 550 and 760  $^\circ\text{C}$ , respectively.

Room temperature photoluminescence (PL) measurements were carried out with a commercial mapper (Philips PLM-150) using an Nd:YAG laser ( $\lambda = 532 \text{ nm}$ ) as an excitation source and an InGaAs array detector. The PL mapping was performed with 1 nm and 10  $\mu\text{m}$  spectral and spatial resolutions, respectively.

Based on an edge-detection algorithm, a custom LabVIEW image recognition software was developed for precise repositioning of samples returning from PL mapping measurements. The software interfaced VIS-CAM and the XYZ-R motorized stage allowing sample reinstallation within 5  $\mu\text{m}$  translational and 0.05 deg rotational accuracies. A schematic idea of the IBESA process is illustrated in Fig. 1. The preliminary results have shown that the investigated InGaAs/InGaAsP microstructure could be blueshifted by 230 nm in a single irradiation step after 30 s irradiation at 780 $^\circ\text{C}$  [27]. These experiments enabled us to determine conditions of irradiation leading to less than 2 nm blueshift in one step.

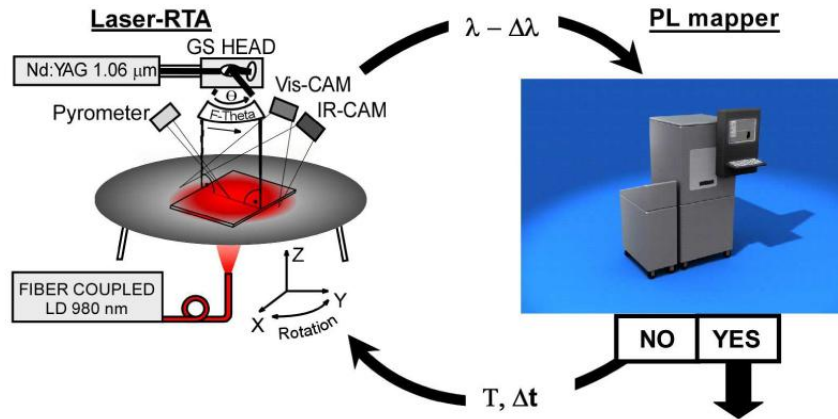


Fig. 1. Schematic idea of the IBESA process.

### 3. Results and discussion

Figure 2(a) shows a PL wavelength peak map of a fragment of the sample irradiated with the Nd:YAG laser beam in 20 sites for different periods of time. The conditions of the irradiation at A1-A4 and B1-B4 sites and the achieved blueshifts are given, respectively, in the ‘Step 1 processing time’ and ‘Peak wavelength’ columns of Table 1. It can be seen that the 30 sec irradiated spots A3 and B1 have been blueshifted by 70 nm from the initial 1550 nm. Their diameter is approximately 280 μm. Figure 2(b) compares PL spectrum of the center of the A3 spot with that of the as-grown material, both obtained under nominally the same excitation conditions. A decreased PL intensity of the A3 site is related to the reduced quantum confinement of the intermixed QWs. It is worth mentioning that for blueshifts ≤ 50 nm the opposite effect was observed, with a slightly increased PL intensity of the intermixed material. A reduced concentration of grown-in defects following the annealing step, before the reduced confinement starts to dominate the QW PL emission intensity, could explain such a behavior.

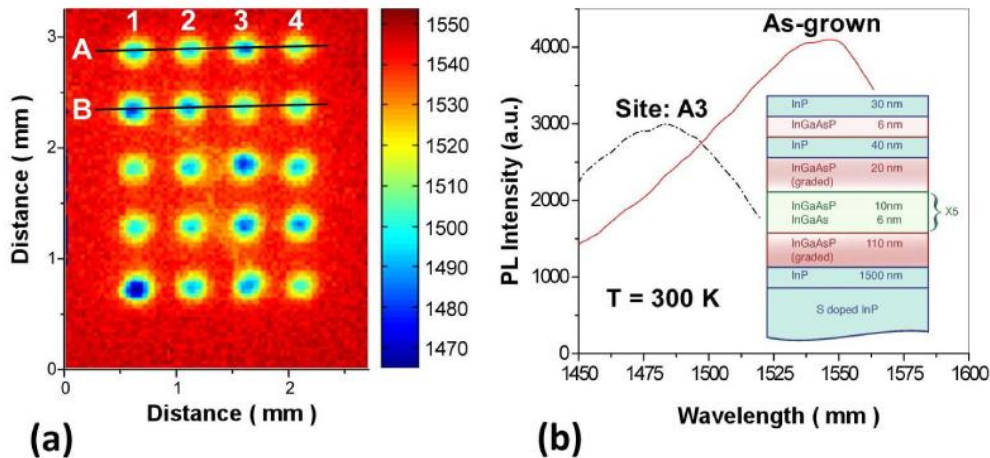


Fig. 2. Photoluminescence PL peak wavelength map of an InGaAs/InGaAsP QW wafer with 20 sites of QW1 material fabricated by Laser-RTA (a), and PL spectra of the as-grown and 70 nm blueshifted (site A3) materials (b). The inset shows details of the processed microstructure.

A similar effect has also been observed in other laser and non-laser annealed InP/InGaAsP QW heterostructures [21,28]. Sites A1, A2 and A4 show the QW material emitting at 1488, 1492 and 1504 nm, while site B2 emits at 1484 and sites B3 and B4 at 1497 nm.

To illustrate the IBESA approach, we requested that all the sites from both rows A and B would emit at 1480 nm, i.e., at the same emission wavelength as A3 and B1. This required additional blueshift amplitudes from 9 to 23 nm. Cross-scans indicating PL peak positions for A series sites, following processing No 1, 2 and 3, are shown in Fig. 3. The targeted 1480 nm emission wavelength was achieved following additional two-step processing at A2 and A4, and one-step at A1. Similarly, as illustrated in Fig. 4, the targeted 1480 nm emission from the B series sites has been achieved following additional one- or two-step-processing. Thus, these results demonstrate a highly reproducible process capable of controlling emission wavelength of InGaAs/InGaAsP QW microstructures, between 1550 and 1480 nm. Depending on the application of the investigated material, this tuning range could easily be extended to 1320 nm. We note that the wavelength tuning precision of  $\pm 1$  nm observed in the current experiment is limited by the relatively low resolution of room-temperature PL spectra. Although for some applications this precision is sufficient, the ultimate tuning precision of the IBESA process will require low-temperature PL data.

**Table 1. Irradiation time and resulting PL peak wavelength emission from InGaAs/InGaAsP QW heterostructures processed by a 3-step IBESA technique.**

Point #	Step 1 processing time (s)	Peak wavelength $\lambda$ (nm)	Step 2 processing time (s)	Peak wavelength $\lambda$ (nm)	Step 3 processing time (s)	Peak wavelength $\lambda$ (nm)
A1	27	1488	-	-	4.5	1479
A2	25	1492	3	1485	2	1480
A3	30	1480	-	-	-	1480
A4	20	1504	9	1486	2	1481
B1	30	1480	-	-	-	1480
B2	28	1484	-	-	1.8	1481
B3	23	1497	4	1486	2.1	1481
B4	23	1497	4	1486	2.1	1481

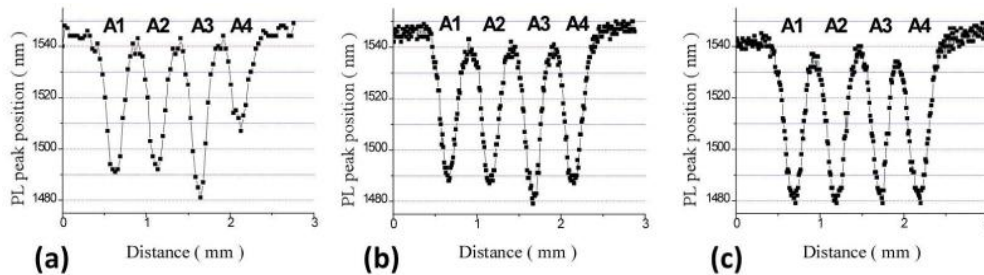


Fig. 3. Photoluminescence peak wavelength cross-scans for A1, A2, A3 and A4 sites following the 1<sup>st</sup> (a), 2<sup>nd</sup> (b) and 3<sup>rd</sup> (c) IBESA annealing step.

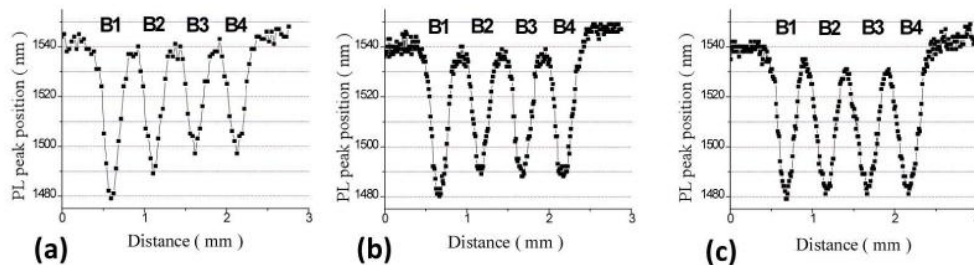


Fig. 4. Photoluminescence peak wavelength cross-scans for B1, B2, B3 and B4 sites following the 1<sup>st</sup> (a), 2<sup>nd</sup> (b) and 3<sup>rd</sup> (c) IBESA annealing step.

## 5. Conclusion

We have investigated the Laser-RTA technique for IBESA of InGaAs/InGaAsP QW wafers originally emitting at 1550 nm. The material blueshifts relatively easily in excess of 230 nm if annealed at 780 °C for 30 sec. To achieve controllable shifts of less than 2 nm, an annealing time shorter than 1-2 sec had to be applied while the annealing temperature was reduced to 760 °C. We have demonstrated that such precision of the annealing time is feasible using the Laser-RTA technique. The IBESA process is carried out in small steps, monitored by taking photoluminescence maps of processed samples. In principle, it should be possible to collect such maps without the need of samples leaving the Laser-RTA processing stage. However, we have developed LabVIEW based software allowing for precise repositioning of the sample returning from PL mapping experiments on the Laser-RTA stage. This allows, for example, carrying out low-temperature PL experiments that are not compatible with the Laser-RTA environment. Targeted values of PL emission wavelength at selected sites of the wafer can be achieved with precision not worse than  $\pm 1$  nm. The position of the laser beam on processed sample is carried out with a galvanometric scanner and an XYZ-R stage that are the permanent features of the Laser-RTA technique. Thus, highly spectrally uniform pixels, lines and circles of the QWI material can be fabricated with this approach. At this stage, tests were performed using only one Nd:YAG laser writing beam, but multi-beam processing should also be possible, which would result in decreased overall processing times.

## Acknowledgements

Funds for this research have been provided by the Natural Sciences and Engineering Research Council of Canada and the Canada Research Chair in Quantum Semiconductors Program (JJD).